Polymer Chemistry

Accepted Manuscript

ROYAL SOCIETY OF CHEMISTRY

www.rsc.org/polymers

Cite this: DOI: 10.1039/c0xx00000x

www.rsc.org/xxxxxx

ARTICLE TYPE

Facile Synthesis of Self-Host Function Iridium Dendrimers Up to Fourth Generation with *N*-phenylcarbazole-Based Polyether Dendrons for Nondoped Phosphorescent Organic Light-Emitting Diodes

Yang Wang [a,b], Shumeng Wang [a,b], Nan Zhao [c], Baoxiang Gao [c], Shiyang Shao [a], Junqiao Ding [a,*], Lixiang Wang [a,*], Xiabin Jing [a], and Fosong Wang [a]

Received (in XXX, XXX) Xth XXXXXXXXX 20XX, Accepted Xth XXXXXXXXX 20XX
DOI: 10.1039/b000000x

Abstract: A facile synthesis has been demonstrated for the first time to construct self-host function Ir-cored dendrimers up to the fourth generation on the basis of a newly developed polyether dendron, where the *N*-phenylcarbazole (NPC) moiety is used as the basic building block instead of benzene so as to improve charge transport while keeping the ease of preparation. With the growing generation number, the dendrimer size can be well tuned in a wide range of 4-10 nm. The obtained fourth generation dendrimer **45NPC-G4** is the largest Ir complex ever reported so far, having a diameter up to 10 nm and a molecular weight as high as 15.9 kDa. Most interestingly, the performance of nondoped phosphorescent organic light-emitting diodes (PhOLEDs) is found to be greatly independent on the molecular size. For example, **9NPC-G2** ($R \approx 30$ Å) reveals the best luminous efficiency as high as 50.5 cd/A (56.6 lm/W, 14.8%), whereas the efficiency of **45NPC-G4** ($R \approx 50$ Å) sharply drops to 10.5 cd/A (5.6 lm/W, 3.4%). The results suggest that an appropriate size of 6 ± 2 nm is desirable to balance the dilemma between luminescent quenching and charge transport, and thereby realize highly efficient nondoped PhOLEDs.

Introduction

Phosphorescent organic light-emitting diodes (PhOLEDs) with transition metal complexes as triplet emitters have attracted much attention since they can harvest both singlet and triplet excitons to realize a theoretical internal quantum efficiency of 100%.[1-6] Among these phosphors, iridium (Ir) complexes show great potential in flat-panel displays and solid-state lightings due to their high photoluminescence quantum yields (PLQYs) and appropriate exciton lifetimes.[7-13] In general, Ir complexes need to be dispersed into a host matrix to inhibit self-quenching caused by strong intermolecular interactions.[14-18] As for this doping technology, phase segregation is an inevitable problem.[19,20] Meanwhile, the doping concentration usually lower than 10 wt% is difficult to be controlled precisely, which may be a significant barrier to reliable and reproducible commercial PhOLEDs.[21-25]

Dendritic architecture presents a promising platform to overcome these issues.[26-28] When an Ir complex is located at the central core, the surrounding dendrons can reduce or even eliminate the luminance quenching so that the formed Ir dendrimers are possible to be used alone as the light-emitting layer to fabricate nondoped PhOLEDs. On the basis of phenylene and Müllen dendrons, such Ir-cored dendrimers were successively demonstrated by P. L. Burn[29-31] and K. Müllen[32] groups to be suitable for nondoped devices. Unfortunately, these dendrons that only consist of benzene units are somewhat electrically insulating to carriers, resulting in unideal nondoped device performance. As an alternative, the electroactive dendron made of carbazole is adopted for the design of multifunctional Ir dendrimers due to its high triplet energy and excellent hole transport capability.[13b,15b] In this case the periphery carbazole dendrons are expected to function as the host for the emissive Ir core, and thereby an efficient self-host system is formed in a single dendritic macromolecule. Up to now, many interesting self-host function Ir dendrimers have been developed within a wide emission color range from blue to red.[33-41] For example, with the second-generation oligocarbazole as the dendron and tris[2-(2,4-difluorophenyl)-pyridyl]iridium as the emissive core, a blue-emitting dendrimer B-G2 was reported to have a unique doping concentration dependence, and its nondoped device gave a maximum luminous efficiency of 31.3 cd/A.[40]

Despite the impressive results, the relationship between dendron generation and nondoped device performance still remains unclear.[30,42] On one hand, the emissive Ir cores are expected to be isolated more and more effectively with the increasing dendron generation, avoiding their interactions that lead to the quenching of the luminance. On the other hand, the large intercore distance would inversely deteriorate charge transport and recombination in a device. That is, an appropriate dendrimer size, in which the luminance quenching can be prevented without a significant reduction of mobility, is desirable to realize efficient nondoped PhOLEDs.

We note that the design and synthesis of different generation dendrimers to control their molecular sizes is a great challenge. Firstly, there lack efficient synthetic routes toward carbazole-containing dendrons. Most of them are synthesized through Pd/Cu-catalyzed Ullmann or Buchwald coupling.[31,32,43,44] As reported in the literatures,[45,46] the metal catalytic activity is greatly influenced by the steric effect, bringing about extremely low yields of high generation dendrons. Secondly, a pre-dendronization method, which involves the preparation of the dendronized ligands followed by the subsequent coordination with Ir salts in polar solvents (glycerol and diglymer etc.), is often utilized to produce Ir dendrimers. However, the large dendronized ligands may possess poor solubility in these polar solvents, leading to incomplete complexation.[33] Therefore, much effort should be paid to explore new strategies for the construction of high-generation dendritic Ir complexes to demonstrate the molecular size effect on the performance of nondoped PhOLEDs.

In this contribution, we report a facile procedure to synthesize self-host function Ir dendrimers up to the fourth generation based on a newly developed polyether dendron made of *N*-phenylcarbazole (NPC). As shown in Fig. 1, the NPC moiety is adopted as the basic building block instead of benzene in a traditional Fréchet dendron. This delicate modification can render the polyether dendron with an interesting electroactive character to some degree, which is beneficial to charge transport in an optoelectronic device. Meanwhile, it can be easily prepared according to the same synthetic route used for Fréchet dendron.[47] Together with a reactive Ir core containing hydroxyl groups, we are able to rapidly construct the first, second, third and even fourth generation Ir dendrimers (3NPC-G1, 9NPC-G2, 21NPC-G3 and 45NPC-G4, Scheme 1) with a controllable molecular size in the range of 4-10 nm. Among them, the fourth generation dendrimer 45NPC-G4 contains 45 NPC units, having a molecular weight as high as 15.9 kDa and a diameter up to 10 nm. To the best of our knowledge, it is the largest dendritic Ir macromolecule reported so far. Most importantly, the relationship between dendrimer size and nondoped device performance has been investigated in detail. It is found that the optimal nondoped device is realized for dendrimer 9NPC-G2 with a suitable diameter of 6 nm to balance the dilemma between luminescent quenching and charge transport, which delivers a state-of-art luminous efficiency of 50.5 cd/A (56.6 lm/W, 14.8%).

Results and Discussion

Synthesis and Characterization

Schemes 2 and 3 outline the synthetic route of the NPC-based polyether dendrons with first to fourth generations. Similar to the Fréchet counterparts,[47] they could be easily synthesized in high yields. At first, (4-(3,6-di-tert-butyl-carbazol-9-yl)phenyl)methanol (D1-OH) and 9-(4-(hydroxymethyl)phenyl)-carbazole-3,6-diol (PC-OH) were prepared as the key building blocks (Scheme 2). Starting from carbazole, the first generation dendron D1-OH was obtained by Friedel-Crafts alkylation,[33] Buchwald C-N coupling[43] and reduction with $NaBH_4$ in sequence. The synthesis of the latter monomer PC-OH was also from carbazole, which was brominated with N-bromosuccinimide (NBS) and further converted into 4 by treatment with CuI and newly prepared solution of sodium methoxide in DMF. Then 4 was transferred to 5 under the same Buchwald C-N coupling conditions. By demethylation of 5 with BBr_3 at 0 °C, 6 was formed accompanied by a benzoic acid byproduct owing to the partly decomposition of methyl benzoate. In order to make use of this byproduct, we directly treated the above unpurified mixture with $LiAlH_4$ in refluxing THF to produce PC-OH in an excellent yield of 96% for two steps.

With D1-OH and PC-OH in hand, the other dendrons D2-OH, D3-OH and D4-OH were then synthesized (Scheme 3). Under the halogenating reagent of CBr_4 in combination with PPh_3, D1-OH was firstly converted into D1-Br, which then reacted with PC-OH via a Williamson reaction[47] to afford D2-OH. This cycle could be repeated to give D3-OH and D4-OH. It should be noted that, the benzyl bromide precusors Dn-Br (n = 1～4) were unstable on silica column, so they were precipitated into methanol and used directly in the next step without further purification. This instability might also be harmful to the etherification, resulting in a low yield for the fourth generation dendron D4-OH (40%). Therefore, a Mistunobu reaction[48] involving benzyl alcohol as the precursor rather than benzyl bromide was adopted for the synthesis of D4-OH, and the yield was further improved to be over 60%.

At the same time, the hydroxyl-functionalized Ir complex core, HO-Ir(pbi)$_3$, was prepared successfully. As shown in Scheme 4, 2-nitroaniline was firstly coupled with 4-iodoanisole through a low temperature Ullmann reaction,[44] followed by reduction with Fe/HCl, amidation with benzoyl chloride, dehydrol cyclization and demethylation with BBr_3. As a consequence, the ligand 11 that contains the reactive hydroxyl group was achieved in a satisfactory overall yield of 67%. Subsequently, a modified two-step procedure,[49] involving the use of silver trifluoroacetate as the promoter to accelerate the coordination reaction, was applied for the ligand 11 to produce HO-Ir(pbi)$_3$ in an isolated yield as high as 80%. Noticeably, this Ir intermediate was dominantly *facial* isomer, whose structure was confirmed by its ^1H NMR spectrum showing only one simple set of signals (Fig. S1†). Moreover, a singlet peak at 10.15 ppm was observed, indicating the existence of the reactive hydroxyl group.

Finally, a Williamson reaction[47] was carried out between Dn-Br (n = 1～4) and HO-Ir(pbi)$_3$ (Scheme 4). In a typical procedure, Cs_2CO_3 and DMF were used as the base and the solvent, respectively. Taking into account that the product solubility was not very good when 21NPC-G3 and 45NPC-G4 were prepared, the mixed solvent of DMF and toluene was employed. Their final purification was conducted by means of gel permeation chromatography (GPC) column separation because of the serious tailing and adsorption on silica column. The resultant Ir dendrimers 3NPC-G1, 9NPC-G2, 21NPC-G3 and 45NPC-G4 were fully characterized by ^1H NMR spectroscopy, MALDI-TOF mass spectrometry, GPC and elemental analysis. As depicted in Fig. S1†, the 10.15 ppm signal corresponding to the hydroxyl group disappears completely, and a characteristic singlet peak is observed at about 8.15 ppm, which originates from the protons at the 4,5-positions of carbazole in the NPC block. These observations imply the successful combination between NPC-based polyether dendrons and Ir core. The MALDI-TOF mass spectrum of every Ir dendrimer shown in Fig. 2 reveals an intense signal from the corresponding molecular ion. Especially, 45NPC-

G4 has a molecular weight of 15.9 kDa, much higher than that of the same generation Ir dendrimer with Müllen dendrons (10.9 kDa).[32] In addition, a narrow polydispersity index (PDI) of 1.09-1.10 is obtained from the GPC characterization for all the dendrimers (Table 1 and Fig. S2†), indicative of their high purity and monodispersity. By comparison to the macromolecules with Fréchet dendrons (PDI = 1.02),[47] a slightly broaden PDI here may be ascribed to the increased rigidity of NPC-based polyether dendrons when NPC is used as the building block in place of benzene.

Thermogravimetric analysis (TGA) and differential scanning calorimetry (DSC) were used to study the thermal properties of the dendrimers (Fig. S3†). They all display good thermal stability with decomposition temperatures (T_d, corresponding to a 5% weight loss) higher than 400 ^oC as well as glass transition temperatures (T_g) higher than 200 ^oC. Additionally, their geometric structures were simulated by PM6 method with Gaussian 09 program package[32], and the *tert*-butyl surface groups were omitted for simplicity. As shown in Scheme 1, the molecular size is well controlled by the dendron generation. For instance, 3NPC-G1 has a diameter of 4 nm, whereas 45NPC-G4 enjoys a diameter up to 10 nm, which marks the birth of the largest Ir dendrimer up to now.

Electrochemical Properties

A. Dendrons. The electrochemical properties of the dendrons D1-OH～D4-OH together with the model compounds G1-Me and MO-G1-Me were firstly explored by cyclic voltammetry (CV) and differential pulse voltammetry (DPV), and the related data are summarized in Table 2 and Table S1. Both D1-OH and G1-Me undergo a reversible oxidation process at a similar potential of about 0.70 V. This process moves negatively towards 0.48 V for MO-G1-Me owing to the stronger electron-donating ability of methoxyl relative to *tert*-butyl substituent. The higher generation dendrons D2-OH～D4-OH all show two successive oxidations at 0.49～0.54 and 0.71～0.72 V, respectively (Fig. 3a). Given the redox behaviors of G1-Me and MO-G1-Me, the former can be safely assigned to the inner NPC with alkyloxy groups, and the latter is related to the outer NPC with *tert*-butyl groups.

It is worthy noting that no oxidation waves can be detected for the Fréchet dendron, Fre-D2-OH, within the same scan range of 0～1.5 V (Fig. S4a†). The difference between Fre-D2-OH and D1-OH～D4-OH clearly illuminates that, unlike the inert nature of Fréchet dendron, the newly developed polyether dendrons that contain NPC block are electroactive indeed. To provide more specific evidence, we fabricated hole-only devices for Fre-D2-OH and D2-OH. As one can see in Fig. 4, Fre-D2-OH shows extremely low conductivity, whereas the current density of D2-OH is increased by about two orders of magnitude. This further suggests that the replacement of benzene by NPC strikingly endows these NPC-based polyether dendrons with an excellent electroactive character, which is responsible for the improved charge-transporting capability.

B. Ir-cored Dendrimers. The corresponding Ir-cored dendrimers all show multiple oxidation processes that can be divided into two parts (Fig. 3b): the first process at 0.18 V arises from Ir core, and the others are attributed to NPC-based polyether dendrons. The signal from Ir core turns out to be weakened in 21NPC-G3 and 45NPC-G4 due to the significant shielding effect from large dendrons. In particular, the oxidation, characteristic of the outer NPC with *tert*-butyl groups, is found to take place at a more positive potential of 0.77～0.82 V in Ir dendrimers compared with pure dendrons (0.71～0.72 V). This is because that the attached Ir core may induce a stabilization of periphery dendrons. According to the first oxidation potential together with the optical band gap (ΔE_g) estimated from the absorption onset, the highest occupied molecular orbit (HOMO) and lowest unoccupied molecular orbit (LUMO) levels are determined to be -4.98 and -2.52 eV for all Ir dendrimers, respectively.

Photophysical Properties

A. Dendrons. The UV-vis absorption and photoluminescence (PL) spectra of the dendrons are shown in Fig. 5a and 5b, respectively. D1-OH displays two main absorption bands at 298 and 347 nm, which can be assigned to the $S_0 \rightarrow S_2$ and $S_0 \rightarrow S_1$ transitions of NPC, respectively.[50] Apart from them, two additional bands appear at 311 and 370 nm for D2-OH～D4-OH. To demonstrate their origin, we compare the absorption spectra of the model compounds G1-Me and MO-G1-Me (Fig. S5†). Consistent with the electrochemical properties, the characteristic absorption is substantially red-shifted from 298/347 nm of G1-Me to 311/370 nm of MO-G1-Me. Hence we can infer that D2-OH～D4-OH possess two sets of bands separately from the outer NPC decorated with *tert*-butyl groups (298/347 nm) and the inner NPC decorated with alkyloxy groups (311/370 nm) because direct electronic communication between different NPC units can hardly happen due to their mutual ether linkage. Furthermore, their corresponding absorption intensity is steadily enhanced with the increasing number of NPC.

Compared with D1-OH (365 nm), the emission maxima of D2-OH～D4-OH are red-shifted to 394 nm. This bathochromic behavior may result from the inner NPC with alkyloxy groups substituted at its 3,6-positions according to the PL difference between G1-Me and MO-G1-Me (Fig. S5†: 366 nm for G1-Me and 394 nm for MO-G1-Me). In addition, no residual emission peaked at 365 nm can be found in the PL spectra of D2-OH～D4-OH when excited at 298 nm, which allows the first excitation of the outer NPC. This means that an efficient Förster energy transfer can happen from the outer NPC to the inner one since there is a good overlap between the absorption of MO-G1-Me and the emission of G1-Me.

B. Ir-cored Dendrimers. The absorption spectra of the Ir-cored dendrimers 3NPC-G1, 9NPC-G2, 21NPC-G3 and 45NPC-G4 are composed of intense UV bands below 400 nm and weak but detectable bands in the visible region of 400-500 nm (Fig. 6a). The UV bands are attributed to spin-allowed ligand-centered (LC) transitions, and the visible bands are related to metal-to-ligand charge-transfer (MLCT) transitions. In particular, the above-mentioned characteristic bands, coming from the NPC-based polyether dendrons, are also observed in the corresponding Ir dendrimers because of the non-conjugated linkage between dendron and core.

As depicted in Fig. 6a, all the dendrimers show the luminance derived from the central emissive Ir core, and their PL spectra in toluene solutions seem to be independent on the generation number. For example, 3NPC-G1 and 45NPC-G4 exhibit the same emission maxima at 515 nm with identical spectral profile. This is reasonable since the dendrons are linked to the emissive core through a non-conjugated ether spacer. In solid states, however, the emission peak is blue-shifted from 540 nm of 3NPC-G1 to 520 nm of 45NPC-G4. Simultaneously, a discernible 0-1 transition appears in Fig. 6b, and thereby a well-resolved structure including 0-0 and 0-1 emissions is measured for 45NPC-G4. These observations are an indicator of the reduced intermolecular interactions between emissive Ir cores in 45NPC-G4 with respect to 3NPC-G1. In fact, the maximum emission of 45NPC-G4 in pure film matches well with that of G0 in dilute solution (517 nm),[33] implying that the fourth dendron could provide the Ir core with a nearly identical environment to the solvent dispersion.

The PLQYs of the dendrimers in solutions were also characterized, and the data are listed in Table 3. They have similar PLQYs of 41～44%, close to that of G0.[33] Interestingly, the estimated film lifetime firstly goes upward from 0.14 μs of 3NPC-G1 to 0.57 μs of 9NPC-G2, and then downward to 0.39 μs of 45NPC-G4 (Fig. S6†). The initial rise from 3NPC-G1 to 9NPC-G2 is related to the decrease of intermolecular interactions induced by the isolation effect. When the dendrimer size further grows, the reduction in the lifetime of 45NPC-G4 is beyond our expectation, and the reason is not very clear now. According to the previous report,[51] we may tentatively ascribe it to a relative large nonradiative decay rate originating from strong vibrational coupling.

Electroluminescent Properties

To investigate the electroluminescent (EL) properties of the dendrimers, nondoped PhOLEDs were fabricated with a configuration of indium tin oxide (ITO)/poly(3,4-ethylenedioxythiophene):poly(styrene sulfonic acid) (PEDOT:PSS) /dendrimers/2,7-bis(diphenylphosphoryl)-9,9’-spirobifluorene (DPSF)/LiF/Al (Fig. S7†). Here DPSF was used as the electron-transporting and hole-blocking material.[52]

The current density and brightness versus voltage, luminous efficiency versus current density curves as well as EL spectra are shown in Fig. 7a-d, and the data are tabulated in Table 4. As can be seen from Fig. 7d, all dendrimers exhibit EL solely from the triplet excited states of the emissive Ir core, identical to their PL counterparts in films. On going from 3NPC-G1 to 45NPC-G4, the corresponding Commission International de L’Eclairege (CIE 1931) coordinates are slightly blue-shifted from (0.38, 0.59) to (0.37, 0.57).

With the increasing dendron generation, reasonably, charges may become more difficult to flux into the emissive Ir core either through a direct injection or through an indirect transport process from periphery dendrons. As a result, the turn-on voltage is found to be increased from 2.4 V of 3NPC-G1 to 5.8 V of 45NPC-G4. Correspondingly, the current density and brightness at the same driving voltage are gradually decreased from 3NPC-G1 to 45NPC-G4 (Fig. 7a-b). Moreover, a maximum brightness of 6260, 3030, 1240 and 660 cd/m^2, a maximum luminous efficiency of 30.7, 50.5, 39.2 and 10.5 cd/A, a maximum power efficiency of 37.3, 56.6, 34.7 and 5.6 lm/W, and a maximum external quantum efficiency (EQE) of 9.1, 14.8, 11.7 and 3.4% are realized for 3NPC-G1, 9NPC-G2, 21NPC-G3 and 45NPC-G4, respectively. The efficiency, especially for 9NPC-G2, is much higher than that of the Müllen-type Ir dendrimers (21.9 cd/A, 6.1%).[32] As discussed above, the unique electroactive feature of NPC-based polyether dendrons may contribute to the improved device performance.

Fig. 8 gives the luminous efficiency as a function of molecular size. With the growing dendrimer size, the efficiency increases to a maximum value for 9NPC-G2 ($R \approx 30$ Å) followed by a significant reduction for 45NPC-G4 ($R \approx 50$ Å). The interesting size dependence is believed to result from the balance between luminescent quenching and charge transport. When the dendrimer is small, carriers are easy to enter into Ir core to produce excitons, and the shielding effect dominates device performance. Therefore, as the generation grows at first, the luminescence quenching can be effectively suppressed, leading to improved luminous efficiency. This result is in good agreement with the trend of film lifetimes. When the dendrimer grows large enough, charge transporting turns out to be more difficult, which is verified by the significant decrease of the hole current (Fig. S9†). Accordingly, the excited excitons could not be formed directly on Ir core, but be generated initially on periphery dendrons and then transferred to Ir core. This means that the formed excitons would have more chance to undergo some nonradiative decay processes, such as conformational distortion and energy relaxation.[53] Furthermore, with the growing generation, the energy transfer from outer dendrons to Ir core also seems to be less efficacious. As a result, 45NPC-G4 shows a sharp drop in device efficiency in comparison to other dendrimers 3NPC-G1, 9NPC-G2 and 21NPC-G3. The same trend has been previously observed in Ir dendrimers containing triphenylamine-based dendrons.[42]

Conclusions

In conclusion, on the basis of a newly developed NPC-containing polyether dendron, we have demonstrated a facile procedure for the synthesis of self-host function Ir dendrimers up to 45NPC-G4, which is the largest dendritic complex ever reported. This type of polyether dendron is basically composed of NPC rather than benzene, and thereby possesses an interesting electroactive character, resulting in the improved hole transporting relative to the Fréchet dendron. Meanwhile, the ease of synthesis, especially for very large dendrons, offers a convenient way to construct different generation Ir dendrimers with varied molecular size from 4 nm of 3NPC-G1 to 10 nm of 45NPC-G4. The tunable molecular size in a wide range of 4-10 nm together with the excellent charge transport capability of periphery dendrons does provide us a unique platform to systematically investigate the molecular size effect on the performance of nondoped PhOLEDs. It is found that the luminous efficiency is firstly up from 30.7 cd/A of 3NPC-G1 ($R \approx 20$ Å) to 50.5 cd/A of 9NPC-G2 ($R \approx 30$ Å), and then down to 39.2 and 10.5 cd/A for 21NPC-G3 ($R \approx 40$ Å) and 45NPC-G4 ($R \approx 50$ Å), respectively. Our results indicate that an optimal dendrimer size may be 6 ± 2 nm since such a size scale can not only prevent intermolecular interaction induced luminescence quenching, but also keep effective charge transport from the dendritic wedge to the central Ir core.

Notes and references

[a] *State Key Laboratory of Polymer Physics and Chemistry, Changchun Institute of Applied Chemistry, Chinese Academy of Sciences, Changchun, 130022, P. R. China E-mail: junqiaod@ciac.ac.cn; lixiang@ciac.ac.cn*
[b] *University of Chinese Academy of Sciences, Beijing, 100049, P. R. China*
[c] *College of Chemistry and Environmental Science, Hebei University, Baoding, 071002, P. R. China*

1. M. A. Baldo, D. F. O'Brien, Y. You, A. Shoustikov, S. Sibley, M. E. Thompson and S. R. Forrest, *Nature*, 1998, **395**, 151.
2. M. A. Baldo, D. F. O'Brien, M. E. Thompson and S. R. Forrest, *Phys. Rev. B*, 1999, **60**, 14422.
3. (*a*) Y. R. Sun, N. C. Giebink, H. Kanno, B. W. Ma, M. E. Thompson and S. R. Forrest, *Nature*, 2006, **440**, 908; (*b*) L. Ying, C. L. Ho, H. B. Wu, Y. Cao and W. Y. Wong, *Adv. Mater.*, 2014, **26**, 2459; (*c*) X. L. Yang, G. J. Zhou and W. Y. Wong, *J. Mater. Chem. C*, 2014, **2**, 1760; (*d*) G. J. Zhou, W. Y. Wong and S. Suo, *J. Photoch. Photobio. C*, 2010, **11**, 133.
4. M. K. Nazeeruddin, R. Humphry-Baker, D. Berner, S. Rivier, L. Zuppiroli and M. Graetzel, *J. Am. Chem. Soc.*, 2003, **125**, 8790.
5. C. Adachi, M. A. Baldo, M. E. Thompson and S. R. Forrest, *J. Appl. Phys.*, 2001, **90**, 5048.
6. (*a*) M. C. Tang, D. P. K. Tsang, M. M. Y. Chan, K. M. C. Wong and V. W. W. Yam, *Angew. Chem. Int. Ed.*, 2013, **52**, 7628; (*b*) W. Y. Wong and C. L. Ho, *J. Mater. Chem.*, 2009, **19**, 4457; (*c*) G. J. Zhou, W. Y. Wong and X. L. Yang, *Chem.-Asian. J.*, 2011, **6**, 1706; (*d*) W. Y. Wong and C. L. Ho, *Coord. Chem. Rev.*, 2009, **253**, 1709.
7. S. Lamansky, P. Djurovich, D. Murphy, F. Abdel-Razzaq, H. E. Lee, C. Adachi, P. E. Burrows, S. R. Forrest and M. E. Thompson, *J. Am. Chem. Soc.*, 2001, **123**, 4304.
8. A. Tsuboyama, H. Iwawaki, M. Furugori, T. Mukaide, J. Kamatani, S. Igawa, T. Moriyama, S. Miura, T. Takiguchi, S. Okada, M. Hoshino and K. Ueno, *J. Am. Chem. Soc.*, 2003, **125**, 12971.
9. W. S. Huang, J. T. Lin, C. H. Chien, Y. T. Tao, S. S. Sun and Y. S. Wen, *Chem. Mater.*, 2004, **16**, 2480.
10. H. J. Bolink, E. Coronado, S. G. Santamaria, M. Sessolo, N. Evans, C. Klein, E. Baranoff, K. Kalyanasundaram, M. Grätzel and M. K. Nazeeruddin, *Chem. Commun.*, 2007, 3276.
11. C. L. Ho, W. Y. Wong, Z. Q. Gao, C. H. Chen, K. W. Cheah, B. Yao, Z. Y. Xie, Q. Wang, D. G. Ma, L. A. Wang, X. M. Yu, H. S. Kwok and Z. Y. Lin, *Adv. Funct. Mater.*, 2008, **18**, 319.
12. H. Fukagawa, K. Watanabe, T. Tsuzuki and S. Tokito, *Appl. Phys. Lett.*, 2008, **93**, 133312.
13. (*a*) T. Sajoto, P. I. Djurovich, A. B. Tamayo, J. Oxgaard, W. A. Goddard and M. E. Thompson, *J. Am. Chem. Soc.*, 2009, **131**, 9813; (*b*) C. L. Ho, Q. Wang, C. S. Lam, W. Y. Wong, D. G. Ma, L. X. Wang, Z. Q. Gao, C. H. Chen, K. W. Cheah and Z. Y. Lin, *Chem.-Asian J.*, 2009, **4**, 89.
14. M. A. Baldo, C. Adachi and S. R. Forrest, *Phys. Rev. B.*, 2000, **62**, 10967.
15. (*a*) C. H. Fan, P. P. Sun, T. H. Su and C. H. Cheng, *Adv. Mater.*, 2011, **23**, 2981; (*b*) C. L. Ho, L. C. Chi, W. Y. Hung, W. J. Chen, Y. C. Lin, H. Wu, E. Mondal, G. J. Zhou, K. T. Wong and W. Y. Wong, *J. Mater. Chem.*, 2012, **22**, 215.
16. Y. T. Tao, Q. A. Wang, C. L. Yang, C. Zhong, J. G. Qin and D. G. Ma, *Adv. Funct. Mater.*, 2010, **20**, 2923.
17. Z. M. Hudson, Z. B. Wang, M. G. Helander, Z. H. Lu and S. N. Wang, *Adv. Mater.*, 2012, **24**, 2922.
18. C. W. Lee and J. Y. Lee, *Adv. Mater.*, 2013, **25**, 5450.
19. H. A. Al Attar and A. P. Monkman, *Adv. Funct. Mater.*, 2006, **16**, 2231.
20. S. Reineke, K. Walzer and K. Leo, *Phys. Rev. B*, 2007, **75**, 125328.
21. T. Tsuzuki, Y. Nakayama, J. Nakamura, T. Iwata and S. Tokito, *Appl. Phys. Lett.*, 2006, **88**, 243511.
22. M. R. Zhu, T. L. Ye, X. He, X. S. Cao, C. Zhong, D. G. Ma, J. G. Qin and C. L. Yang, *J. Mater. Chem.*, 2011, **21**, 9326.
23. H. H. Chou and C. H. Cheng, *Adv. Mater.*, 2010, **22**, 2468.
24. S. O. Jeon, S. E. Jang, H. S. Son and J. Y. Lee, *Adv. Mater.*, 2011, **23**, 1436.
25. K. S. Yook and J. Y. Lee, *Org. Electron.*, 2011, **12**, 1711.
26. (*a*) S. H. Hwang, C. N. Moorefield and G. R. Newkome, *Chem. Soc. Rev.*, 2008, **37**, 2543; (*b*) G. J. Zhou, W. Y. Wong, B. Yao, Z. Y. Xie and L. X. Wang, *Angew. Chem. Int. Ed.*, 2007, **46**, 1149.
27. S. C. Lo and P. L. Burn, *Chem. Rev.*, 2007, **107**, 1097.
28. A. W. Freeman, S. C. Koene, P. R. L. Malenfant, M. E. Thompson and J. M. J. Fréchet, *J. Am. Chem. Soc.*, 2000, **122**, 12385.
29. S. C. Lo, T. D. Anthopoulos, E. B. Namdas, P. L. Burn and I. D. W. Samuel, *Adv. Mater.*, 2005, **17**, 1945.
30. S. C. Lo, R. N. Bera, R. E. Harding, P. L. Burn and I. D. W. Samuel, *Adv. Funct. Mater.*, 2008, **18**, 3080.
31. S. C. Lo, R. E. Harding, C. P. Shipley, S. G. Stevenson, P. L. Burn and I. D. W. Samuel, *J. Am. Chem. Soc.*, 2009, **131**, 16681.
32. T. S. Qin, J. Q. Ding, L. X. Wang, M. Baumgarten, G. Zhou and K. Müllen, *J. Am. Chem. Soc.*, 2009, **131**, 14329.
33. J. Q. Ding, J. Gao, Y. X. Cheng, Z. Y. Xie, L. X. Wang, D. G. Ma, X. B. Jing and F. S. Wang, *Adv. Funct. Mater.*, 2006, **16**, 575.
34. J. Q. Ding, J. H. Lu, Y. X. Cheng, Z. Y. Xie, L. X. Wang, X. B. Jing and F. S. Wang, *Adv. Funct. Mater.*, 2008, **18**, 2754.
35. J. Q. Ding, B. Wang, Z. Y. Yue, B. Yao, Z. Y. Xie, Y. X. Cheng, L. X. Wang, X. B. Jing and F. S. Wang, *Angew. Chem. Int. Et.*, 2009, **48**, 6664.
36. J. Q. Ding, J. H. Lu, Y. X. Cheng, Z. Y. Xie, L. X. Wang, X. B. Jing and F. S. Wang, *J. Organomet. Chem.*, 2009, **694**, 2700.
37. L. C. Chen, Z. H. Ma, J. Q. Ding, L. X. Wang, X. B. Jing and F. S. Wang, *Chem. Commun.*, 2011, **47**, 9519.
38. L. C. Chen, Z. H. Ma, J. Q. Ding, L. X. Wang, X. B. Jing and F. S. Wang, *Org. Electron.*, 2012, **13**, 2160.
39. W. W. Tian, C. Yi, B. Song, Q. Qi, W. Jiang, Y. P. Zheng, Z. J. Qi and Y. M. Sun, *J. Mater. Chem. C*, 2014, **2**, 1104.
40. D. B. Xia, B. Wang, B. Chen, S. M. Wang, B. H. Zhang, J. Q. Ding, L. X. Wang, X. B. Jing and F. S. Wang, *Angew. Chem. Int. Ed.*, 2014, **53**, 1048.
41. T. Tsuzuki, N. Shirasawa, T. Suzuki, S. Tokito, *Jpn. J. Appl. Phys.*, 2005, **44**, 4151.
42. M. R. Zhu, J. H. Zou, X. He, C. L. Yang, H. B. Wu, C. Zhong, J. G. Qin and Y. Cao, *Chem. Mater.*, 2012, **24**, 174.
43. K. A. Knights, S. G. Stevenson, C. P. Shipley, S. C. Lo, S. Olsen, R. E. Harding, S. Gambino, P. L. Burn and I. D. W. Samuel, *J. Mater. Chem.*, 2008, **18**, 2121.
44. K. Albrecht and K. Yamamoto, *J. Am. Chem. Soc.*, 2009, **131**, 2244.
45. A. Hameurlaine and W. Dehaen, *Tetrahedron Lett.*, 2003, **44**, 957.
46. A. Kimoto, J. S. Cho, M. Higuchi and K. Yamamoto, *Macromolecules*, 2004, **37**, 5531.
47. C. J. Hawker and J. M. J. Fréchet, *J. Am. Chem. Soc.*, 1990, **112**, 7638.
48. Y. Feng, Y. M. He, L. W. Zhao, Y. Y. Huang and Q. H. Fan, *Org. Lett.*, 2007, **9**, 2261.
49. K. M. Jung, K. H. Kim, J. I. Jin, M. J. Cho and D. H. Choi, *J. Polym. Sci., Part A Polym. Chem.*, 2008, **46**, 7517.
50. C. C. Lee, M. K. Leung, P. Y. Lee, T. L. Chiu, J. H. Lee, C. Liu and P. T. Chou, *Macromolecules*, 2012, **45**, 751.
51. R. E. Harding, S. C. Lo, P. L. Burn and I. D. W. Samuel, *Org. Electron.*, 2008, **9**, 377.
52. K. S. Yook, S. E. Jang, S. O. Jeon and J. Y. Lee, *Adv. Mater.*, 2010, **22**, 4479.
53. K. R. J. Thomas, A. L. Thompson, A. V. Sivakumar, C. J. Bardeen and S. Thayumanavan, *J. Am. Chem. Soc.*, 2005, **127**, 373.

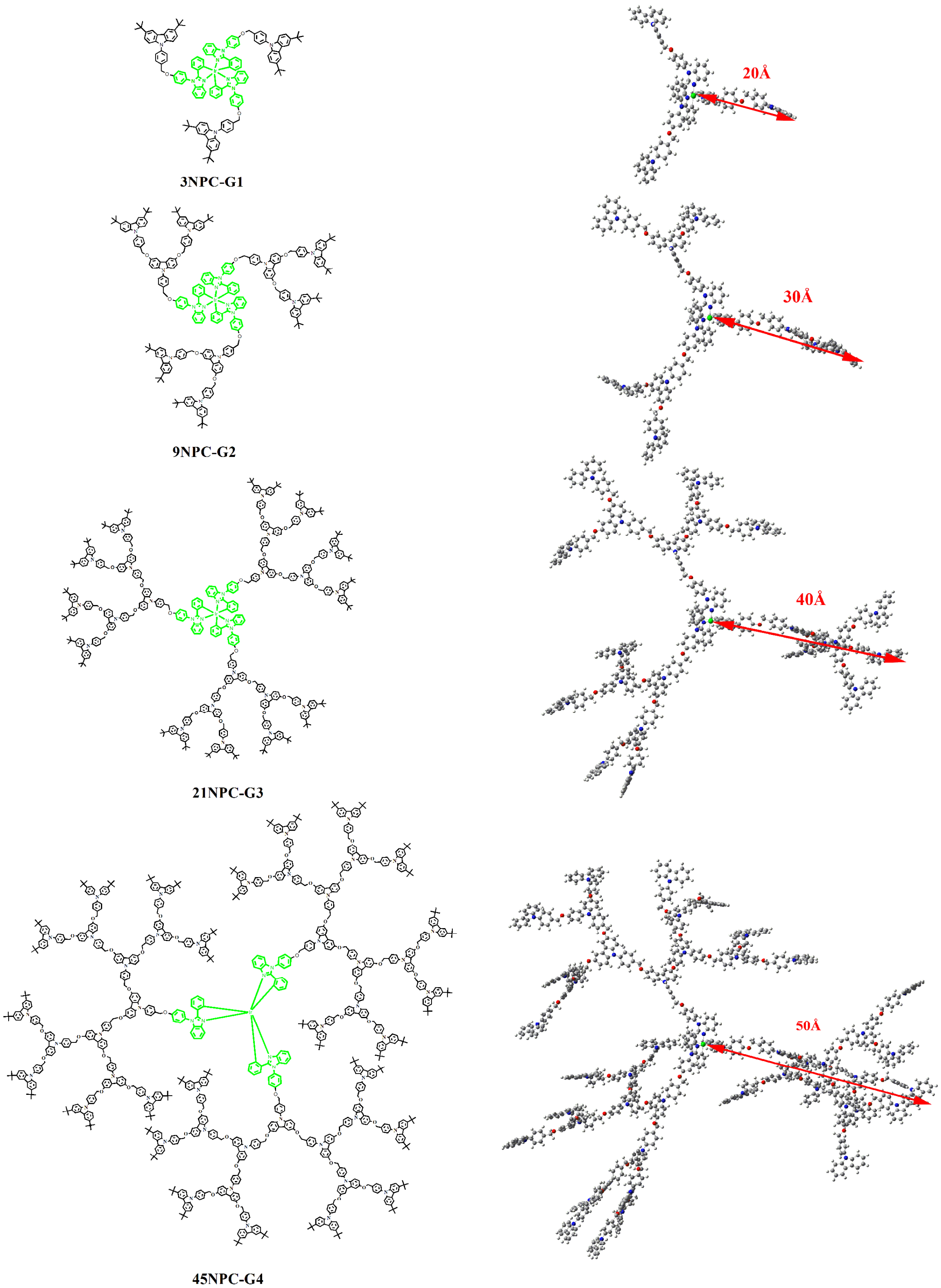

Scheme 1. Molecular structures and sizes of Ir-cored dendrimers.

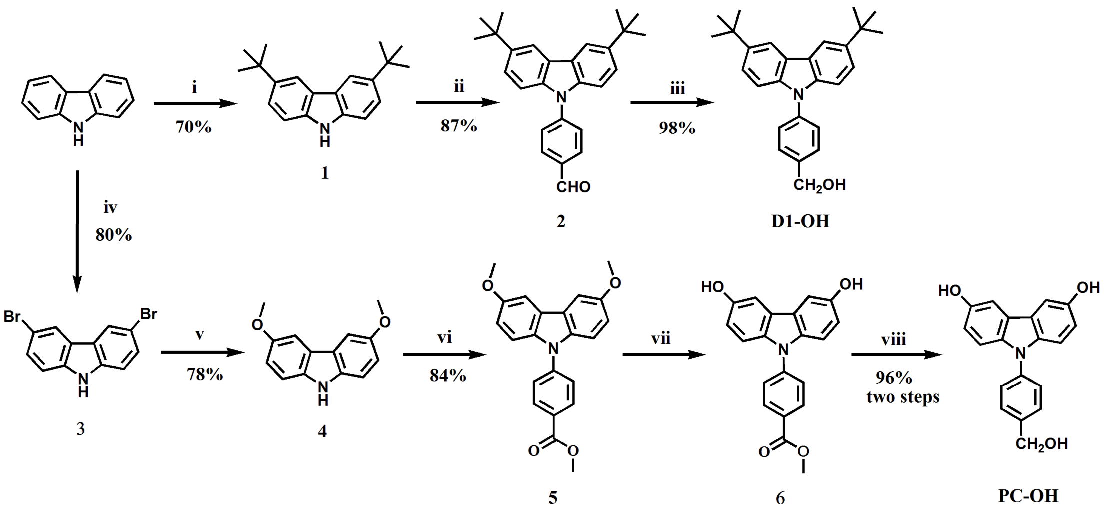

Scheme 2. Synthesis of the first generation dendron **D1-OH** and monomer **PC-OH**. Reagents and conditions: (i) *t*-BuCl , $ZnCl_2$, CH_3NO_2, CH_2Cl_2, room temperature; (ii) 4-bromobenzaldehyde, $Pd(OAc)_2$, $P(t\text{-}Bu)_3$, K_2CO_3, toluene, reflux; (iii) $NaBH_4$, ethanol/THF, room temperature; (iv) NBS, DMF, 0 °C; 5 (v) CH_3ONa, CuI, DMF, reflux; (vi) methyl 4-bromobenzoate, $Pd(OAc)_2$, $P(t\text{-}Bu)_3$, K_2CO_3, toluene, reflux; (vii) BBr_3, CH_2Cl_2, 0 °C; (viii) $LiAlH_4$, THF, reflux.

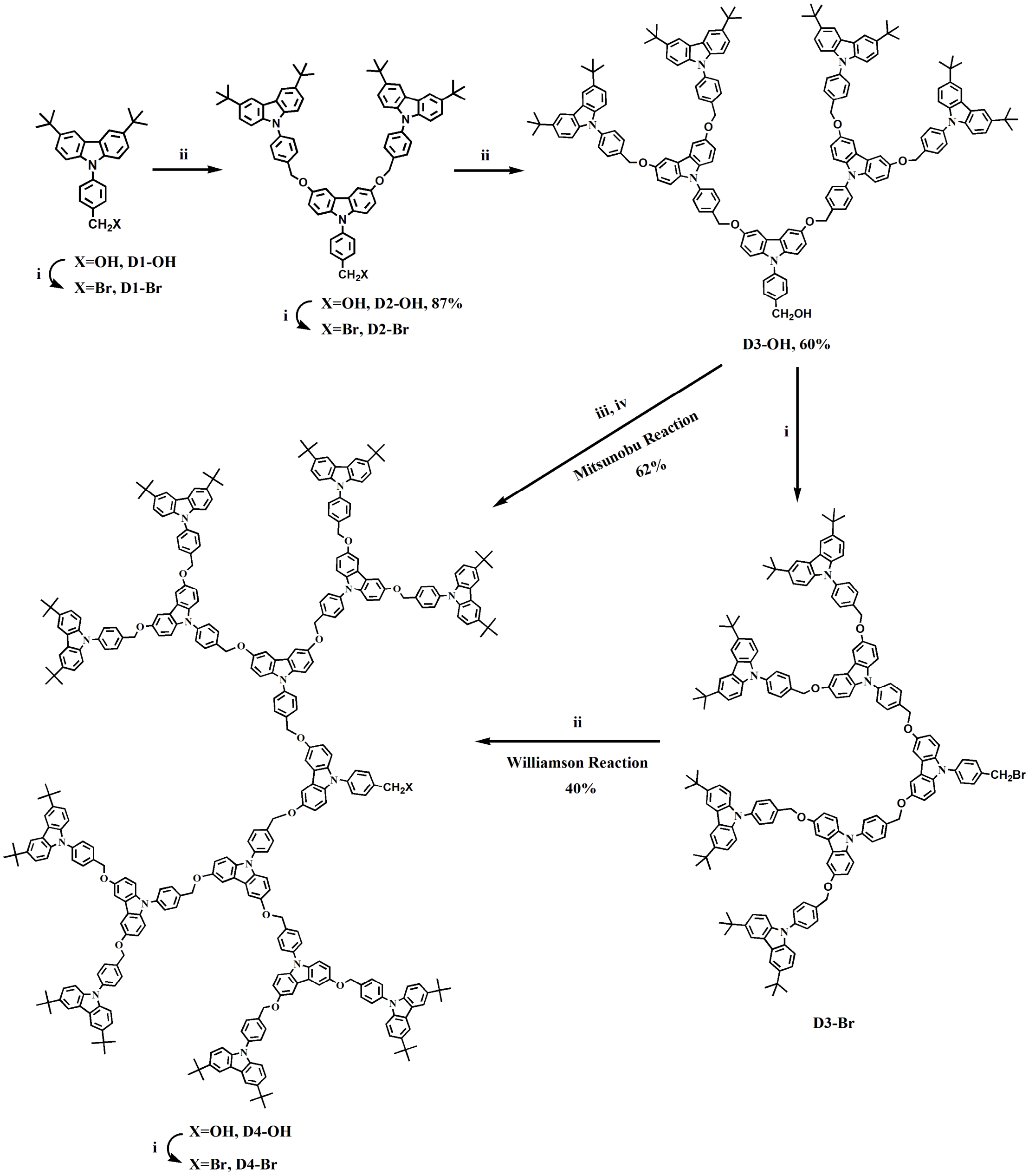

Scheme 3. Synthesis of higher generation dendrons **D2-OH**, **D3-OH** and **D4-OH**. Reagents and conditions: (i) CBr_4, PPh_3, CH_2Cl_2, room temperature; (ii) **PC-OH**, K_2CO_3, 18-crown-6, acetone, reflux; (iii) **6**, DIAD, PPh_3, THF, room temperature; (iv) $LiAlH_4$, THF, reflux.

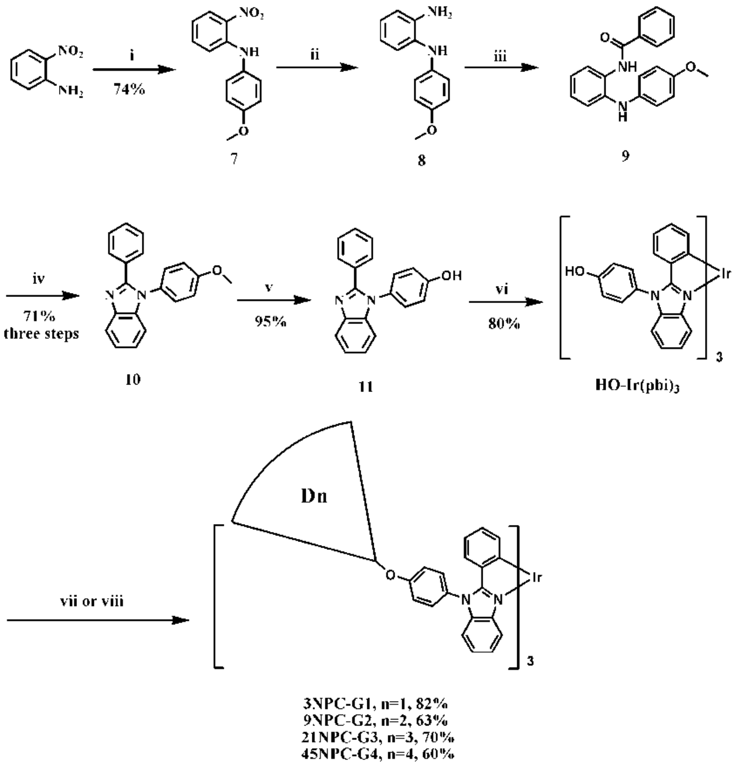

Scheme 4. Synthesis of Ir-cored dendrimers. Reagents and conditions: (i) 4-iodoanisole, CuI, *trans*-1,2-cyclohexanediamine, K_3PO_4, toluene, reflux; (ii) Fe, HCl, methanol/water, reflux; (iii) benzoyl chloride, Et_3N, 0 °C; (iv) CH_3COOH, reflux; (v) BBr_3, CH_2Cl_2, 0 °C; (vi) iridium(III) chloride trihydrate, water, 2-methoxyethanol, reflux, and then silver trifluoroacetate, **11**, 2-ethoxyethanol, reflux; (vii) **Dn-Br**, Cs_2CO_3, DMF, 100 °C, n = 1 and 2; (viii) **Dn-Br**, Cs_2CO_3, DMF/toluene, 100 °C, n = 3 and 4.

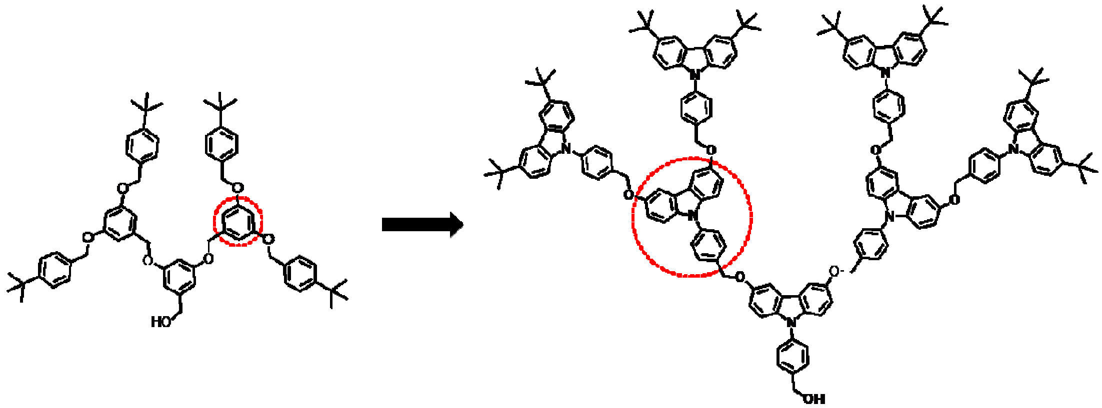

Fig. 1 Design of NPC-based polyether dendrons that combine ease of preparation and electroactive character.

5

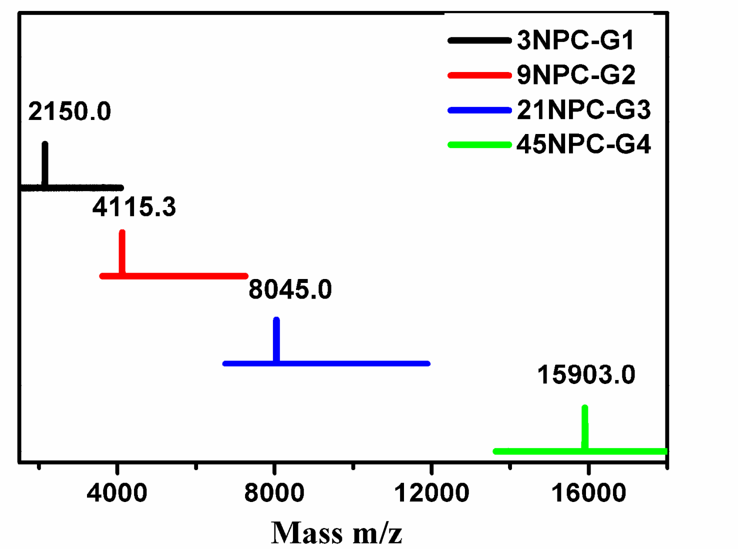

Fig. 2 MALDI-TOF mass spectra of Ir dendrimers.

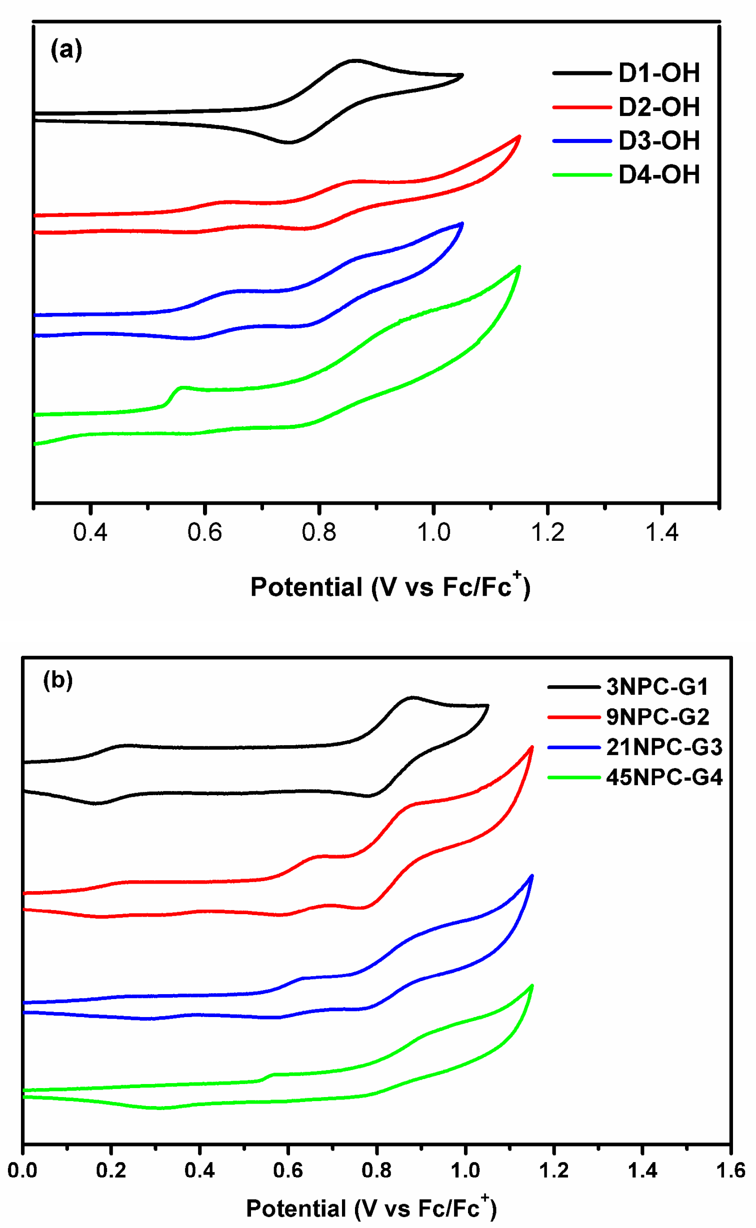

Fig. 3 Cyclic voltammograms of dendrons **D1-OH**～**D4-OH** (a) and their corresponding Ir dendrimers (b).

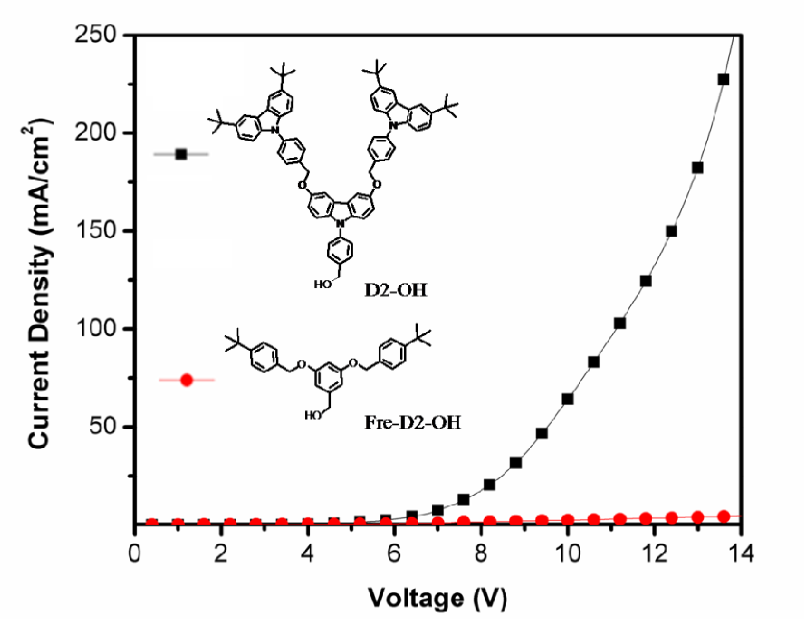

Fig. 4 Current density — voltage characteristics of hole-only devices for **D2-OH** and **Fre-D2-OH**.

5

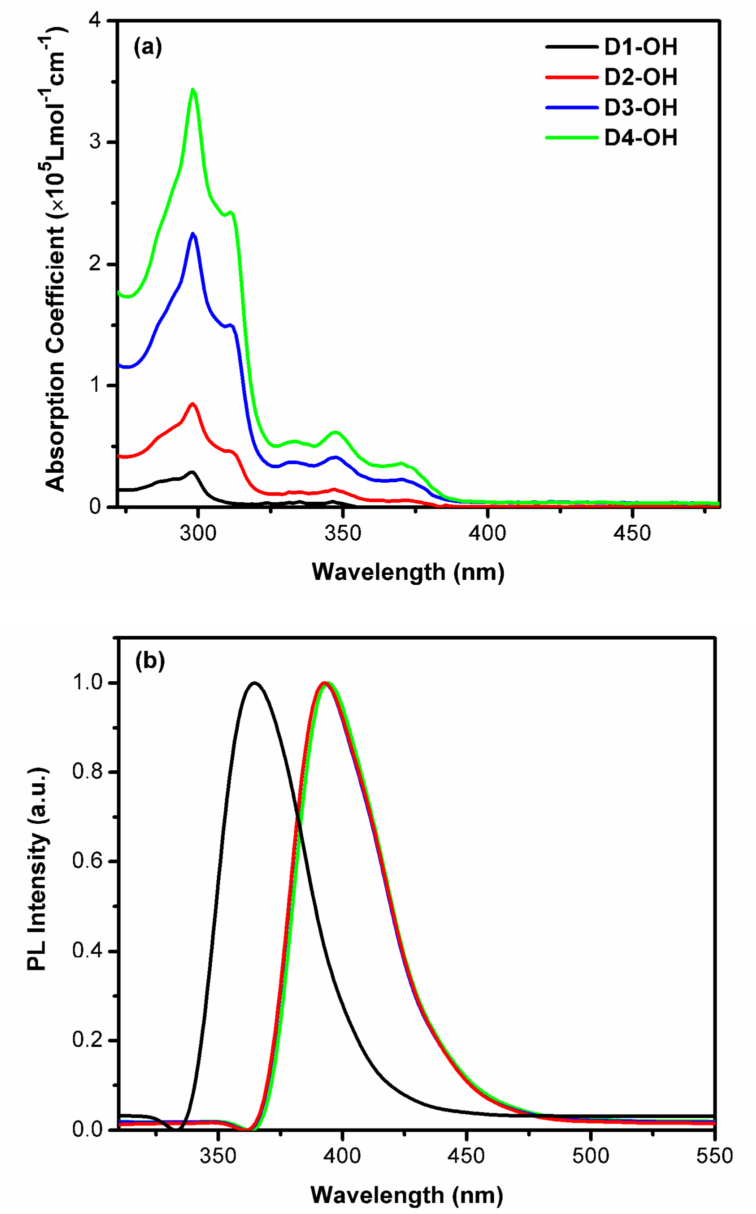

Fig. 5 UV-vis absorption (a) and PL spectra in solutions (b) for dendrons **D1-OH**～**D4-OH**.

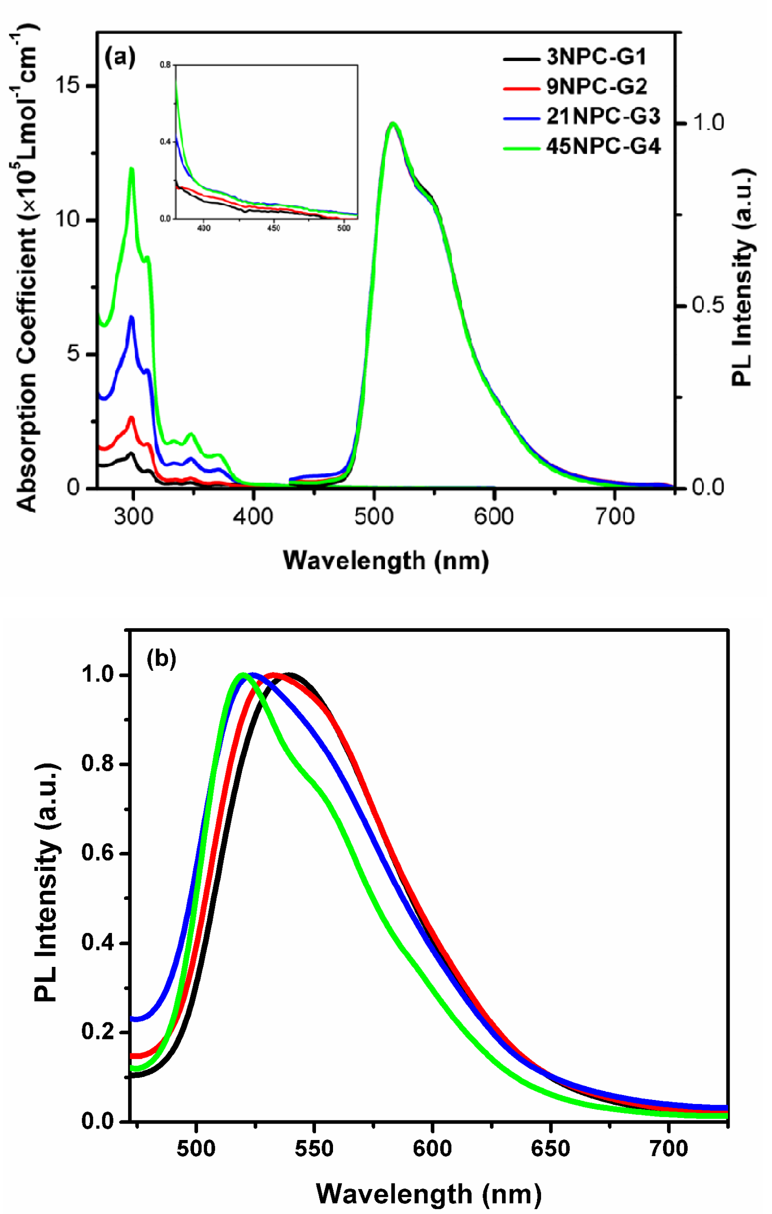

Fig. 6 (a) UV-vis absorption and PL spectra in solutions of Ir dendrimers (λ_{ex} = 412 nm). (b) PL spectra in thin films of Ir dendrimers (λ_{ex} = 412 nm).

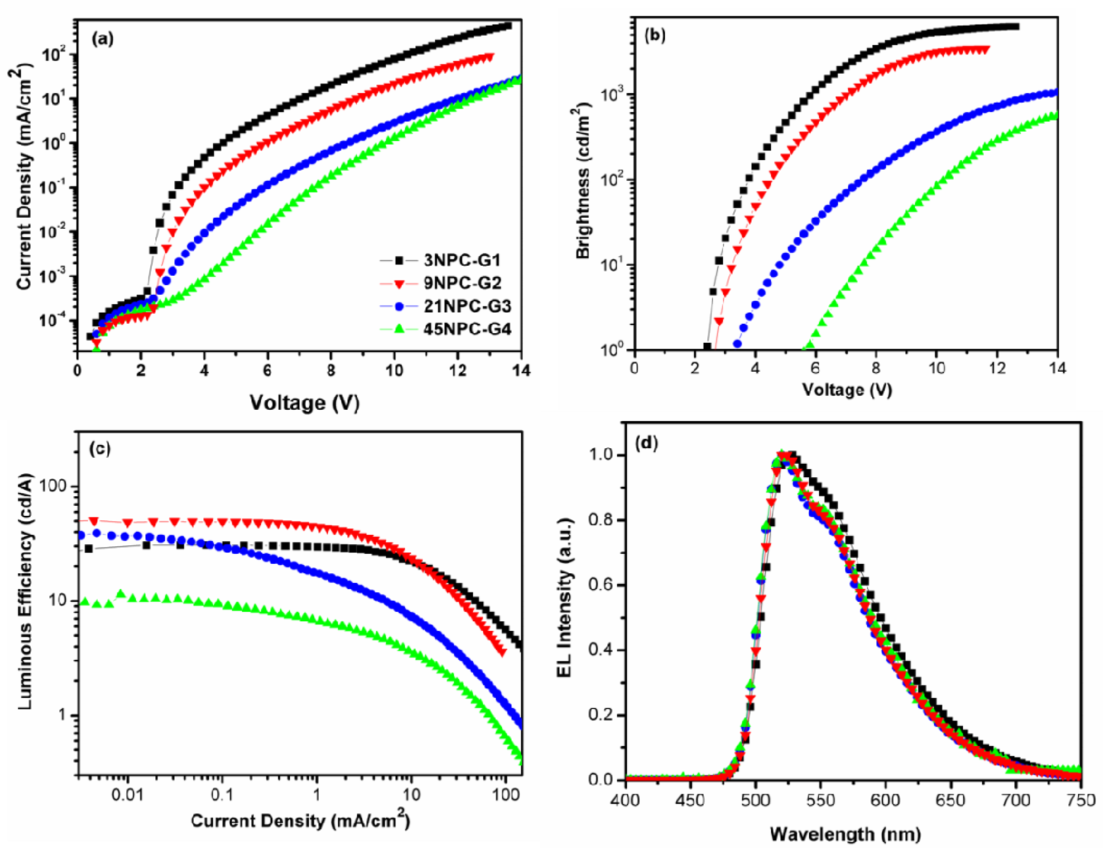

Fig. 7 Current density versus voltage (a), brightness versus voltage (b), luminous efficiency versus current density (c), and EL spectra at 9 V (d) for Ir dendrimers.

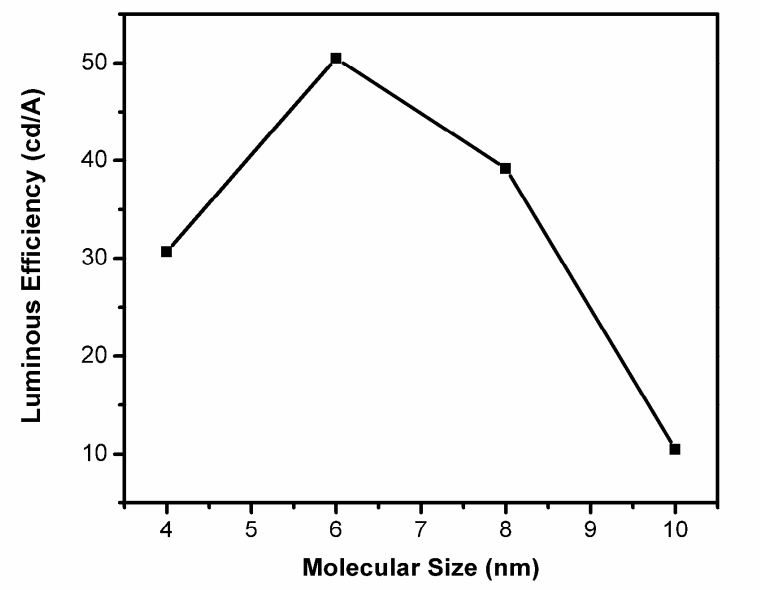

Fig. 8 The molecular size dependence of luminous efficiency.

Table 1. Molecular weights, diameters and thermal properties of Ir dendrimers.

	M [a] [g/mol]	M_{MS} [b] [g/mol]	M_n [c] [g/mol]	PDI [c]	D [d] [Å]	T_d [e] [ºC]	T_g [e] [ºC]
3NPC-G1	2149.9	2150.0	2119	1.09	40	408	229
9NPC-G2	4115.3	4115.3	5598	1.09	60	436	243
21NPC-G3	8044.3	8044.5	9267	1.10	80	451	244
45NPC-G4	15902.4	15903.0	14581	1.10	100	418	241

[a] Molar mass of dendrimers. [b] Measured by MALDI-TOF mass spectrometry. [c] Measured by GPC equipped with refractive index detector and with polystyrene as standard. [d] Calculated by PM6 method. [e] Scan rate: 10 ºC/min.

Table 2. Electrochemical properties of dendrons and their corresponding dendrimers.

	$E_{1/2,\mathrm{ox}}$ [a] [V vs Fc/Fc$^+$]	HOMO [b] [eV]	ΔE_g [c] [eV]	LUMO [d] [eV]
D1-OH	0.72			
D2-OH	0.54, 0.73			
D3-OH	0.53, 0.72			
D4-OH	0.49, 0.60			
3NPC-G1	0.17, 0.78	-4.97	2.46	-2.51
9NPC-G2	0.18, 0.62, 0.77	-4.98	2.46	-2.52
21NPC-G3	0.18, 0.40, 0.61, 0.82	-4.98	2.46	-2.52
45NPC-G4	0.18, 0.40, 0.56, 0.78	-4.98	2.46	-2.52

[a] Measured in DCM solutions. The half-wave potential given is taken from differential pulse voltammetry peaks; [b] HOMO = -e(E_{ox} + 4.8 V), where E_{ox} is the first oxidation peak of $E_{1/2,\mathrm{ox}}$; [c] ΔE_g is the optical bandgap estimated from the absorption onset; [d] LUMO = HOMO + ΔE_g.

Table 3. Photophysical properties of dendrons and their corresponding dendrimers.

	λ_{abs} ($\log\varepsilon$) [a] [nm]	λ_{em} [b] [nm]	λ_{em} [c] [nm]	Φ_{PL} [d] [%]	τ_{av} [e] [μs]
D1-OH	298(4.5), 347(3.6)	365			
D2-OH	298(4.9), 311(4.7), 347(4.2), 370(3.7)	394			
D3-OH	298(5.3), 311(5.2), 347(4.6), 370(4.4)	394			
D4-OH	298(5.5), 311(5.4), 347(4.8), 370(4.6)	394			
3NPC-G1	298(5.1), 312(4.8), 347(4.3), 376(4.2), 412(3.9), 452(3.5), 490(2.9)	515	540	43	0.14
9NPC-G2	298(5.4), 312(5.2), 348(4.6), 369(4.3), 412(3.4), 450(3.7), 490(3.2)	515	532	44	0.57
21NPC-G3	298(5.8), 312(5.6), 348(5.0), 371(4.9), 412(4.1), 451(3.9), 490(3.6)	515	524	42	0.50
45NPC-G4	298(6.1), 312(5.9), 348(5.3), 370(5.1), 412(4.1), 452(3.9), 490(3.5)	515	520	41	0.39

[a] Measured in DCM at 298 K with a concentration of 10^{-6} M; [b] Measured in toluene at 298 K with a concentration of 10^{-5} M; [c] Measured in films; [d] Measured in degassed toluene at 298 K relative to *fac*-Ir(ppy)$_3$ (Φ = 0.40) and the excitation wavelength is 412 nm; [e] Measured in films at 298 K and the lifetimes are obtained as an average value by a biexponential fit of emission decay curves.

Table 4. Performance of nondoped devices based on Ir dendrimers.

	V_{on} ^{a} [V]	$\eta_{ext,\ max}$ [%]	$\eta_{c,\ max}$ [cd/A]	$\eta_{p,\ max}$ [lm/W]	η_{ext} ^{b} [%]	η_{c} ^{b} [cd/A]	η_{p} ^{b} [lm/W]	λ_{em} [nm]	CIE ^{c} (x,y)
3NPC-G1	2.4	9.1	30.7	37.3	9.0	30.3	25.1	528	(0.38, 0.58)
9NPC-G2	2.8	14.8	50.5	56.6	13.3	48.5	33.1	524	(0.37, 0.59)
21NPC-G3	3.4	11.7	39.2	34.7	6.3	21.3	8.8	520	(0.37, 0.59)
45NPC-G4	5.8	3.4	10.5	5.6	1.8	6.0	1.8	520	(0.37, 0.57)

[a] At a brightness of 1 cd/m^2; [b] At a brightness of 100 cd/m^2; [c] At a voltage of 9 V. η_{ext}, external quantum efficiency; η_{c}, luminous efficiency; η_{p}, power efficiency.

Table of Contents

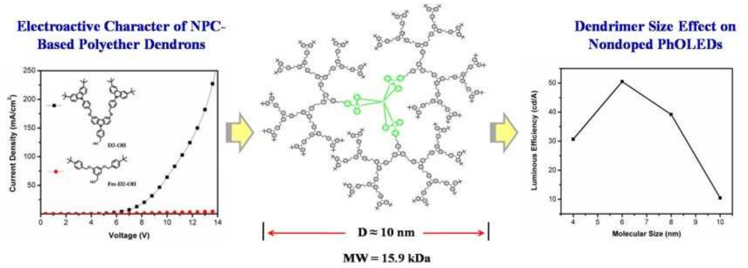

Self-host functional iridium dendrimers up to fourth generation with *N*-phenylcarbazole-based polyether dendrons have been developed for the application in nondoped PhOLEDs.

Graphical Abstract

Facile Synthesis of Self-Host Function Iridium Dendrimers Up to Fourth Generation with *N*-phenylcarbazole-Based Polyether Dendrons for Nondoped Phosphorescent Organic Light-Emitting Diodes

Yang Wang a,b, Shumeng Wang a,b, Nan Zhao c, Baoxiang Gao c, Shiyang Shao a, Junqiao Ding a,*, Lixiang Wang a,*, Xiabin Jing a, and Fosong Wang a

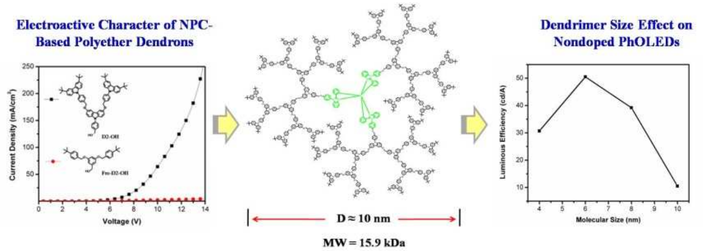

A facile synthesis has been demonstrated for the first time to construct self-host function Ir-cored dendrimers up to the fourth generation on the basis of a newly developed polyether dendron, where the *N*-phenylcarbazole (NPC) moiety is used as the basic building block instead of benzene so as to improve charge transport while keeping the ease of preparation. With the growing generation number, the dendrimer size can be well tuned in a wide range of 4-10 nm. The obtained fourth generation dendrimer **45NPC-G4** is the largest Ir complex ever reported so far, having a diameter up to 10 nm and a molecular weight as high as 15.9 kDa. Most interestingly, the performance of nondoped phosphorescent organic light-emitting diodes (PhOLEDs) is found to be greatly independent on the molecular size. For example, **9NPC-G2** ($R \approx 30$ Å) reveals the best luminous efficiency as high as 50.5 cd/A (56.6 lm/W, 14.8%), whereas the efficiency of **45NPC-G4** ($R \approx 50$ Å) sharply drops to 10.5 cd/A (5.6 lm/W, 3.4%). The results suggest that an appropriate size of 6 ± 2 nm is desirable to balance the dilemma between luminescent quenching and charge transport, and thereby realize highly efficient nondoped PhOLEDs.